

# SPDC: once again on the parameters of transverse entanglement outside the near zone.

M.V. Fedorov<sup>1,2\*</sup> and S.S. Mernova<sup>1,2</sup>, K.V. Sliporod<sup>1,2</sup>

<sup>1</sup>*A.M. Prokhorov General Physics Institute, Russian Academy of Sciences, Moscow, Russia*

<sup>2</sup>*National Research University Higher School of Economics, Moscow, Russia*

(Dated: March 2, 2021)

As known, the degree of entanglement of biphoton states with respect to the transverse components of photon wave vectors (momenta) or coordinates can be characterized either by the parameter  $K$  associated with the Schmidt decompositions, or by the parameter  $R$ , defined as the ratio of the widths of the unconditional and conditional single-particle distributions of biphoton states. As entanglement is a fundamental characteristics of a state, it must be independent of a choice of its different representations, i.e. its entanglement parameters must be identical in the coordinate and momentum representations. Likewise, entanglement itself and its characterization parameters must remain constant along the photon propagation length. It's known, however, that only the parameter  $K$  obeys these requirements, whereas the parameter  $R$  in the coordinate representation deviates from  $K$  beyond the near zone and, thus, becomes inapplicable as a measure of the degree of entanglement. But, as shown below, there is a way of saving the parameter  $R$  by means of modifying its definition in such a way that the modified parameter  $R$  turns out to be as good as the parameter  $K$  both in the momentum and coordinate representations, as well as in the near and far zones and everywhere between them. We will discuss also possible ways of measuring this newly defined parameter  $R$  experimentally.

## 1. INTRODUCTION

One of the simplest regimes of Spontaneous Parametric Down-Conversion (SPDC) is the collinear, frequency-degenerate regime with the type-I phase-matching. In this regime the pump propagates in the nonlinear crystal as an extraordinary wave whereas emitted photons are of the ordinary-wave type, and a scheme of the SPDC process is  $e \rightarrow o + o$ . In this case the arising biphoton states can be entangled in spectral or/and angular variables of emitted photons. Very often these two types of entanglement can be considered independently of each other. In this work we will consider only angular or transverse entanglement, where the often used name “transverse” is related to the fact that propagation angles of emitted photons are determined by components of their wave vectors  $\mathbf{k}_{1,2\perp}$ , perpendicular to the central propagation direction  $Oz$  of both the pump and emitted photons. The transverse-variable wave function of the arising biphoton state is pretty well known [1, 2] to be given by

$$\Psi(\mathbf{k}_1, \mathbf{k}_2) \propto \exp\left[-\frac{(\mathbf{k}_{1\perp} + \mathbf{k}_{2\perp})^2 w^2}{4}\right] \times \text{sinc}\left[\frac{L\lambda_p}{8\pi n_o}(\mathbf{k}_{1\perp} - \mathbf{k}_{2\perp})^2\right]. \quad (1)$$

The first term on right-hand side of this equation is the transverse profile of the pump with  $w$  being its waist, and the second term characterizes formation of the biphoton beam in the crystal, and in this expression  $\text{sinc}(u) = \sin u/u$ ,  $L$  is the crystal length along the  $z$ -direction,  $n_o$  is the ordinary-wave refractive index, and

$\lambda_p$  is the wavelength of the pump. Most often the normalization coefficient in front of the wave function (1) is not important and for this reason it's dropped and replaced by the proportionality symbol. The same will be done in most of cases below. Some special situations when normalization factors are important will be explicitly noted and explained.

Concerning Eq. (1), note that it does not take into account rather important walk-off effects arising owing to anisotropy of the pump refractive index, though these factors can affect significantly features of transverse distributions of emitted photons and the degree of transverse entanglement [3?]. Manifestations of the walk-off effects are most important for emitted photons with wave vectors located in the plane containing the optical axis of a crystal. It's assumed below that this optical-axis plane is  $(y, z)$  and it is located vertically. On the opposite, for photons propagating in the plane  $(x, z)$  perpendicular to  $(y, z)$  the walk-off effect does not exist. For this reason we will consider here only this simplest case, when wave vectors of the pump and of emitted-photons are located in the horizontal observation plane  $(x, z)$ . In experiment such selection can be provided by an appropriately installed slit after the nonlinear crystal. As for the expression for the biphoton transverse wave function (1), after selection it takes the form

$$\Psi(k_{1x}, k_{2x}) \propto \exp\left[-\frac{(k_{1x} + k_{2x})^2 w^2}{4}\right] \Psi(k_{1x}, k_{2x}) \times \text{sinc}\left[\frac{L\lambda_p}{8\pi n_o}(k_{1x} - k_{2x})^2\right]. \quad (2)$$

In addition to this momentum wave function, one can consider also the coordinate biphoton wave function de-

\*Electronic address: fedorovmv@gmail.com

defined as the Fourier transformation of  $\Psi(k_{1x}, k_{2x})$ :

$$\tilde{\Psi}(x_1, x_2) = \int dk_{1x} dk_{2x} e^{i(x_1 k_{1x} + x_2 k_{2x})} \Psi(k_{1x}, k_{2x}), \quad (3)$$

where  $x_1$  and  $x_2$  are the transverse coordinates of photons in the  $(x, z)$  plane.

For analytical calculations the sinc-function in Eqs. (1), (2) is modeled often by the Gaussian function, with which the wave function of Eq. (2) takes the double-Gaussian form

$$\Psi_{2G}(k_{1x}, k_{2x}) \propto \exp\left[-\frac{(k_{1x} + k_{2x})^2 a^2}{2}\right] \times \exp\left[-\frac{(k_{1x} - k_{2x})^2 b^2}{2}\right], \quad (4)$$

where  $a = w/\sqrt{2}$  and  $b = \sqrt{0.38L\lambda_p/4\pi n_o}$  with the coefficient 0.38 found from the condition that the FWHMs of the sinc- and Gaussian functions coincide:  $\text{FWHM}[\text{sinc}(u^2)] \approx \text{FWHM}[\exp(-0.38u^2)]$ .

For the double-Gaussian wave function of Eq. (4) its Fourier transformation (3) is easily performed to give the following double-Gaussian wave function in the coordinate representation:

$$\tilde{\Psi}_{2G}(x_1, x_2) \propto \exp\left[-\frac{(x_1 + x_2)^2}{2a^2}\right] \exp\left[-\frac{(x_1 - x_2)^2}{2b^2}\right]. \quad (5)$$

Parameters characterizing the degree of entanglement for double-Gaussian wave functions are also well known (see e.g. [4]). One of them is the parameter  $K$  related to the Schmidt decomposition [5]. The simplest way of its calculation is the direct four-fold integration of the product of wave functions either in the momentum or coordinate representation

$$K_k^{-1} = \int dk_{1x} dk'_{1x} dk_{2x} dk'_{2x} \tilde{\Psi}_{2G}(k_{1x}, k_{2x}) \tilde{\Psi}_{2G}^*(k'_{1x}, k'_{2x}) \times \tilde{\Psi}_{2G}^*(k_{1x}, k'_{2x}) \tilde{\Psi}_{2G}(k'_{1x}, k_{2x}) \quad (6)$$

and

$$K_x^{-1} = \int dx_1 dx'_1 dx_2 dx'_2 \tilde{\Psi}_{2G}(x_1, x_2) \tilde{\Psi}_{2G}^*(x'_1, x'_2) \times \tilde{\Psi}_{2G}^*(x_1, x'_2) \tilde{\Psi}_{2G}(x'_1, x_2). \quad (7)$$

Note that the subscripts  $k$  and  $x$  in Eqs. (6), (7) and henceforth refer, respectively, to the momentum and coordinate representations. Note also that for calculation of the Schmidt entanglement parameters  $K$  via the integrated products of wave functions, the latter have to be unit-normalized. The results of integrations in Eqs. (6) and (7) are identical, and the Schmidt entanglement parameters both in the momentum and coordinate representations are given by [6]

$$K_k = K_x = \frac{a^2 + b^2}{2ab}. \quad (8)$$

An alternative parameter characterizing the degree of entanglement is the ratio of widths of unconditional and conditional single-particle probability distributions [7]. For the double-Gaussian wave functions the unconditional single-particle distributions are defined as

$$\frac{dW^{(u.c.)}(k_{1x})}{dk_{1x}} = \int dk_{2x} |\Psi(k_{1x}, k_{2x})|^2 \quad (9)$$

and

$$\frac{dW^{(u.c.)}(x_1)}{dx_1} = \int dx_2 |\tilde{\Psi}(x_1, x_2)|^2, \quad (10)$$

where “*u.c.*” means unconditional. Let the widths of these curves be  $\Delta k_1^{u.c.}$  and  $\Delta x_1^{u.c.}$ .

As for the conditional distributions, they are defined even much simpler

$$\frac{dW_k^{(c)}(k_{1x})}{dk_{1x}} = |\Psi_k(k_{1x}, 0)|^2 \quad (11)$$

and

$$\frac{dW^{(c)}(x_1)}{dx_1} = |\tilde{\Psi}_x(x_1, 0)|^2, \quad (12)$$

and let the widths of these curves be  $\Delta k_1^{(c)}$  and  $\Delta x_1^{(c)}$ . Then the definitions of the parameter  $R$  in the momentum and coordinate representations are

$$R_k = \frac{\Delta k_1^{(u.c.)}}{\Delta k_1^{(c)}} \quad \text{and} \quad R_x = \frac{\Delta x_1^{(u.c.)}}{\Delta x_1^{(c)}}. \quad (13)$$

With the use of the model double-Gaussian wave functions (4) and (5), the widths of unconditional and conditional single-particle distributions and are easily found to be given by

$$\Delta k_1^{(u.c.)} = \frac{1}{\Delta x_1^{(c)}} = \frac{\sqrt{a^2 + b^2}}{ab} \quad \text{and} \quad (14)$$

$$\Delta k_1^{(c)} = \frac{1}{\Delta x_1^{(u.c.)}} = \frac{2}{\sqrt{a^2 + b^2}}. \quad (15)$$

The reproduced here reciprocity relations between the momentum and coordinate conditional and unconditional widths [6] confirm immediately the well known identity of the entanglement parameters  $K$  and  $R$  valid for both momentum and coordinate representations

$$R_k = R_x = K_k = K_x = \frac{a^2 + b^2}{2ab}. \quad (16)$$

However, as shown in the works [8] and [9], in application to biphoton beams propagating in free space after formation in the nonlinear crystal, because of diffraction, the formulated conclusion is correct absolutely only in the near zone, but beyond this zone it becomes wrong for the parameter  $R$  in the coordinate representation. This is the case to be discussed below.

## 2. DIFFRACTION

For the diffraction effects to be taken into account in the paraxial approximation, the wave functions of Eqs. (2), (4) have to be completed with the propagation factor

$$\exp\{i[(k_{1z} + k_{2z})z - 2\omega t]\} \approx \exp\left[i\frac{2\pi}{\lambda_p}(z - ct)\right] \times \exp[-i\zeta(k_{1x}^2 + k_{1x}^2)], \quad (17)$$

where

$$\zeta = \frac{z\lambda_p}{2\pi}. \quad (18)$$

With the most important last factor on the right-hand side of Eq. (17) taken into account, the double-Gaussian wave functions (4) and (5) take the form

$$\Psi_{2G}(k_{1x}, k_{2x}; \zeta) \propto \exp\left[-\frac{(k_{1x} + k_{2x})^2(a^2 + i\zeta)}{2}\right] \times \exp\left[-\frac{(k_{1x} - k_{2x})^2(b^2 + i\zeta)}{2}\right], \quad (19)$$

and

$$\tilde{\Psi}_{2G}(x_1, x_2; \zeta) \propto \exp\left[-\frac{(x_1 + x_2)^2}{2(a^2 + i\zeta)}\right] \exp\left[-\frac{(x_1 - x_2)^2}{2(b^2 + i\zeta)}\right]. \quad (20)$$

If  $\zeta \neq 0$ , in all formulas (6), (7), (9)-(12) the wave functions  $\Psi_{2G}(k_{1x}, k_{2x})$  (4) and  $\tilde{\Psi}_{2G}(x_1, x_2)$  (5) must be replaced by  $\Psi_{2G}(k_{1x}, k_{2x}; \zeta)$  (19) and  $\tilde{\Psi}_{2G}(x_1, x_2; \zeta)$  (20). However, for the parameters  $K_k$ ,  $R_k$  and  $K_x$  this replacement will not change their values compared to the case  $\zeta = 0$ . This is almost evident for the momentum-representation parameters  $K_k$  and  $R_k$ : after substitution into Eq. (6) of  $\Psi_{2G}(k_{1x}, k_{2x}; \zeta)$  instead of  $\Psi_{2G}(k_{1x}, k_{2x})$  all imaginary parts of phases in four times repeated wave functions compensate each other which makes the parameter  $K_k$  independent of  $\zeta$ . For the parameter  $R_k$ , the same conclusion is even more evident. As both the unconditional and conditional distributions (9), (11) are determined by the squared absolute values of the corresponding wave functions, and as in the momentum representation  $|\Psi_{2G}(k_{1x}, k_{2x}; \zeta)| \equiv |\Psi_{2G}(k_{1x}, k_{2x}; 0)|$ , evidently, the same is true for the parameter  $R_k$ :  $R_k(\zeta) \equiv R_k(0)$ .

Less evident but also provable (see section 3 below) is the missing influence of diffraction on the Schmidt entanglement parameter  $K_x$  (7) in the coordinate representation, owing to which both in the near zone and beyond

$$K_k = R_k = K_x = \frac{a^2 + b^2}{2ab} \quad \text{at any } \zeta. \quad (21)$$

Thus, the only parameters which can be modified owing to diffraction are the conditional and unconditional

single-photon distributions in the coordinate representation, their widths and the parameter  $R_x$ . Direct calculations with the use of the wave function (20) and definitions (13) give the following results

$$\Delta x_1^{(u.c.)}(\zeta) = \frac{\sqrt{(a^2 + b^2)(a^2 b^2 + \zeta^2)}}{2ab}, \quad (22)$$

$$\Delta x_1^{(c)}(\zeta) = \sqrt{\frac{(a^4 + \zeta^2)(b^4 + \zeta^2)}{(a^2 + b^2)(a^2 b^2 + \zeta^2)}}, \quad (23)$$

and

$$R_x(\zeta) = \frac{a^2 + b^2}{2ab} \frac{\sqrt{(a^4 + \zeta^2)(b^4 + \zeta^2)}}{a^2 b^2 + \zeta^2}. \quad (24)$$

The second fraction on the right-hand side of Eq. (24) makes the parameter  $R_x(\zeta)$  depending on the propagation distance  $z$  and differs it from the ideal values of other entanglement parameters (21). Typical pictures of the dependencies  $\Delta x_1^{(u.c.)}(\zeta)$ ,  $\Delta x_1^{(c)}(\zeta)$  and  $R_x(\zeta)$  are shown in Fig. 1.

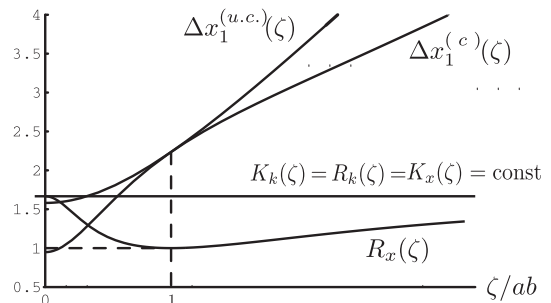


Figure 1: Found with the use of the wave function  $\tilde{\Psi}_{2G}(x_1, x_2; \zeta)$  (20) widths of the unconditional and conditional single-particle distributions and their ratio - parameter  $R_x(\zeta)$  vs.  $\zeta$  (18);  $\Delta x_1^{(u.c.)}$  and  $\Delta x_1^{(c)}$  are in units of  $\sqrt{a^2 + b^2}$  and, as an example, the ratio  $a/b$  is taken equal 3.

This picture and equations (22)-(24) agree with the results and conclusions of the works [8, 9], and thus, indeed, in contrast to other parameters,  $K_k$ ,  $R_k$  and  $K_x$ , the parameter  $R_x$  cannot serve as a reliable entanglement parameter beyond the near zone.

It's a pity. But it raises other questions. E.g., whether it's possible to modify in any way the definition of the width-ratio parameter to return it to the group of reliable entanglement parameters both for the near zone and beyond? And if yes, then where is such new width-ratio parameter "hidden"? And how can it be measured? Some answers to these question are given in the next sections.

## 3. THE REDUCED DENSITY MATRIX AND A NEW WIDTH-RATIO PARAMETER

A quick answer for one of the asked questions is very simple: information about all correlations, entanglement

and characterizing them parameters is accumulated in the reduced density matrix, for the state with the wave function  $\Psi_{2G}(x_1, x_2; \zeta)$  (20) defined as

$$\rho_r(x_1, x'_1) = \int dx_2 \tilde{\Psi}_{2G}(x_1, x_2; \zeta) \tilde{\Psi}_{2G}^*(x'_1, x_2; \zeta). \quad (25)$$

Not dwelling upon details of integration and transformations, let us show the final result:

$$\rho_r(x_1, x'_1) = N \exp \left\{ -\frac{1}{a^2 b^2 + \zeta^2} \left[ \frac{a^2 b^2}{a^2 + b^2} (x_1 + x'_1)^2 + \frac{a^2 + b^2}{4} (x_1 - x'_1)^2 + i\zeta (x_1^2 - x'^2_1) \right] \right\}, \quad (26)$$

where the factor  $N$ ,

$$N = \frac{2ab}{\sqrt{\pi} \sqrt{(a^2 b^2 + \zeta^2)(a^2 + b^2)}}, \quad (27)$$

provides the unit normalization of the reduced density matrix:  $\text{Tr} \rho_r = \int dx_1 \rho_r(x_1, x_1) = 1$ . Moreover, as known [4, 5] and as it can be confirmed by direct integrations, the trace of the squared reduced density matrix equals the inverse value of the Schmidt entanglement parameter  $K_x^{-1}$ :

$$\frac{1}{K_x} = \text{Tr}(\rho_r^2) = \int dx_1 dx_2 |\rho_r(x_1, x_2)|^2 = \frac{2ab}{a^2 + b^2}. \quad (28)$$

The remarkable feature of the reduced density matrix (26) is that its imaginary part, or phase, turns zero if  $x_1^2 = x'^2_1$ , i.e., in two cases: if  $x'_1 = x_1$  or if  $x'_1 = -x_1$ . In these two cases the reduced density matrix takes the form of two different single-particle distributions, along the counterdiagonal line in the  $(x_1, x'_1)$  plane,  $\rho_r(x_1, x_1)$ , and along the main diagonal,  $\rho_r(x_1, -x_1)$ . The counterdiagonal distribution has the form:

$$\begin{aligned} \frac{dW_+^{(\rho_r)}(x_1; \zeta)}{dx_1} &= \rho_r(x_1, x_1; \zeta) = \int dx_2 |\tilde{\Psi}_{2G}(x_1, x_2; \zeta)|^2 = \\ &= N \exp \left\{ -\frac{4a^2 b^2}{(a^2 b^2 + \zeta^2)(a^2 + b^2)} x_1^2 \right\}. \end{aligned} \quad (29)$$

This distribution coincides with the  $\zeta$ -dependent unconditional single-particle distribution, found from the wave function (19), and the width of the distribution (29) coincides with  $\Delta x_1^{(u.c.)}(\zeta)$  (22)

$$\Delta x_1^{(+)}(\zeta) = \Delta x_1^{(u.c.)}(\zeta) = \frac{\sqrt{(a^2 + b^2)(a^2 b^2 + \zeta^2)}}{2ab}. \quad (30)$$

The main-diagonal single-particle distribution accumulated in the reduced density matrix occurs at  $x_1 + x'_1 = 0$  and is given by

$$\begin{aligned} \frac{dW_-^{(\rho_r)}(x_1; \zeta)}{dx_1} &= \rho_r(x_1, -x_1; \zeta) = \\ &= \int dx_2 \tilde{\Psi}_{2G}(x_1, x_2; \zeta) \tilde{\Psi}_{2G}^*(-x_1, x_2; \zeta) = \\ &= N \exp \left\{ -\frac{a^2 + b^2}{a^2 b^2 + \zeta^2} x_1^2 \right\}. \end{aligned} \quad (31)$$

The width of this new single-particle distribution is

$$\Delta x_1^{(-)}(\zeta) = \sqrt{\frac{a^2 b^2 + \zeta^2}{a^2 + b^2}}. \quad (32)$$

The ratio of widths of these two single-particle distributions (29) and (31) can be considered as the new width-ratio entanglement parameter

$$R_{new} = R_{diag} = \frac{\Delta x_1^{(+)}(\zeta)}{\Delta x_1^{(-)}(\zeta)} = \frac{a^2 + b^2}{2ab}. \quad (33)$$

Remarkably enough, the parameter  $R_{new}$  is independent of  $\zeta$ , i.e., it is valid and keeps the same form both in near and far zones, as well as everywhere between them. And, besides, in contrast to  $R_x$  (24), the parameter  $R_{new}$  coincides with the other parameters of the degree of transverse entanglement,  $R_{new} = R_k = K_x = K_k$ . It's worth noting that independence of the parameter  $R_{new}$  of  $\zeta$  contrasts with the behavior of the widths  $\Delta x_1^{(+)}(\zeta)$  and  $\Delta x_1^{(-)}(\zeta)$  which are growing functions of  $\zeta$  shown in Fig. 2.

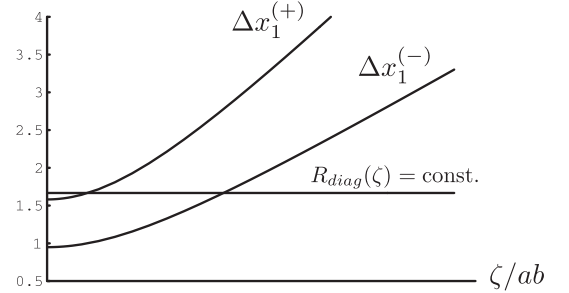


Figure 2: The widths  $\Delta x_1^{(+)}$  and  $\Delta x_1^{(-)}$  vs.  $\zeta$  and their ratio  $R_{diag} = \Delta x_1^{(+)} / \Delta x_1^{(-)}$ ; as well as in Fig.1,  $\Delta x_1^{(+)}$  and  $\Delta x_1^{(-)}$  are in units of  $\sqrt{a^2 + b^2}$  and the ratio  $a/b$  is taken equal 3.

As it's seen clearly, in both of these two widths the dependence on  $\zeta$  is present. But in both of them it is determined only by the same simple factor  $\sqrt{a^2 b^2 + \zeta^2}$ , and this factor disappears in the ratio of widths  $\Delta x_1^{(+)} / \Delta x_1^{(-)} = R_{new}$ . A side remark is that the  $\zeta$ -dependence of the widths  $\Delta x_1^{(+)}$  and  $\Delta x_1^{(-)}$  violates the reciprocity relations between the momentum and coordinate uncertainties (15) [6], which turns out to be valid in the case of transverse entanglement only in the near zone.

#### 4. MEASUREMENTS

The suggested above new entanglement parameter and the given demonstration of its features are simple enough and hardly can raise any doubts themselves. But it's true that the presented derivations were based on modeling the sinc-function in Eq. (2) by the Gaussian function and, subsequently, on the use of the model double-Gaussian coordinate wave function  $\tilde{\Psi}_{2G}(x_1, x_2; \zeta)$  (20).

Without these simplifications it's impossible to derive analytical expressions for the  $x_{1,2}$ - and  $z$ -dependent biphoton wave function and reduced density matrix. Numerical simulations can help in principle but they are difficult too and are not done yet. In this situation experimental measurement of the distribution  $\rho_r(x_1, -x_1)$  would be most appropriate for clarifying whether the theoretical conclusions based on the Gaussian modeling remain valid even beyond this assumption or not, and in particular, whether the width of this distribution  $\Delta x_-(\zeta)$  is similar to or different from that of the above-derived expression (32).

Without Gaussian modeling, we can use only the general definition of the momentum wave function in the near zone  $\Psi(k_{1x}, k_{2x})$  (2), its beyond-near-zone extension  $\Psi(k_{1x}, k_{2x}; \zeta) = \Psi(k_{1x}, k_{2x}) \times \exp[-i\zeta(k_{1x}^2 + k_{2x}^2)]$  and the general form the Fourier transformation (3) to the coordinate wave function  $\tilde{\Psi}(x_1, x_2; \zeta)$ . The non-Gaussian reduced density matrix is defined as

$$\begin{aligned} \rho_r(x_1, x'_1; \zeta) &= \int dx_2 \tilde{\Psi}(x_1, x_2; \zeta) \tilde{\Psi}^*(x'_1, x_2; \zeta) = \\ &= \int dx_2 |\tilde{\Psi}(x_1, x_2; \zeta)| |\tilde{\Psi}^*(x'_1, x_2; \zeta)| \times \\ &\quad \times e^{i[\varphi(x_1, x_2; \zeta) - \varphi(x'_1, x_2; \zeta)]}, \end{aligned} \quad (34)$$

where  $\varphi(x_1, x_2; \zeta)$  and  $\varphi(x'_1, x_2; \zeta)$  are phases of the corresponding biphoton wave functions.

Eq. (34) shows explicitly that for measuring the reduced density matrix one has to measure first both absolute values and phases of the wave functions, and knowledge of phases  $\varphi(x_1, x_2; \zeta)$  of the biphoton wave function will be crucially important for further summation over  $x_2$ . This contrasts with the often accepted assumption that the total phase of the biphoton wave function as whole is unimportant at all and does not affect any physically measurable quantities. As we see, this is not true for the reduced density matrix.

Absolute values of the coordinate wave function,  $|\tilde{\Psi}(x_1, x_2; \zeta)|$ , can be measured rather easily in a traditional way of splitting the beam of biphotons for two channels and measuring coincidence signals by two detector, one in the upper and one in the lower channels, with varying locations of detectors, which gives

$$|\tilde{\Psi}(x_1, x_2; \zeta)| \propto \sqrt{N(x_1, x_2; \zeta)}, \quad (35)$$

where  $N(x_1, x_2; \zeta)$  is the number of detector counts per given time at given locations of detectors. These measurements are sufficient for finding the counterdiagonal single-particle distribution

$$\rho_r(x_1, x_1) = \sum_{x_2} N(x_1, x_2; \zeta), \quad (36)$$

where the sum over  $x_2$  imitates integration. As for the main-diagonal single-particle distribution determined by the reduced density matrix, in terms of measured absolute

values of the wave function it is given by

$$\begin{aligned} \rho_r(x_1, -x_1; \zeta) &= \sum_{x_2} \sqrt{N(x_1, x_2; \zeta) N(-x_1, x_2; \zeta)} \times \\ &\quad \times \exp\{i[\varphi(x_1, x_2; \zeta) - \varphi(-x_1, x_2; \zeta)]\}, \end{aligned} \quad (37)$$

and in this case measurement of phases of the wave function is needed and is unavoidable.

In principle, various aspects of similar problems were discussed in a number of works [10–17]. Not pretending for giving here an overview of these works or adapting any of their methods to our goals, we describe below a scheme of measurements which seems to us to be most appropriate for finding phases of the wave function under consideration.

But note first that in the momentum representation the transverse wave function (2) is even in its dependence on the sum and difference of variables,  $k_{1x} \pm k_{2x}$ , and hence,  $\Psi(k_{1x}, k_{2x}; \zeta) = \Psi(-k_{1x}, -k_{2x}; \zeta)$ . Because of this, the same feature is shared also by the double Fourier transform of the wave function:  $\tilde{\Psi}(x_1, x_2; \zeta) = \tilde{\Psi}(-x_1, -x_2; \zeta)$ . With the use of this feature and the definition of the Fourier transformation, we get

$$\begin{aligned} [\tilde{\Psi}(x_1, x_2; \zeta)]^* &= \tilde{\Psi}(-x_1, -x_2; -\zeta) = \tilde{\Psi}(x_1, x_2; -\zeta) \quad \text{or} \\ \tilde{\Psi}(x_1, x_2; -\zeta) &= |\tilde{\Psi}(x_1, x_2; \zeta)| e^{-i\varphi(x_1, x_2; \zeta)}. \end{aligned} \quad (38)$$

With this remark taken into account, a scheme for measuring phases  $\varphi(x_1, x_2; \zeta)$  can be suggested to have the form described in Fig. 3.

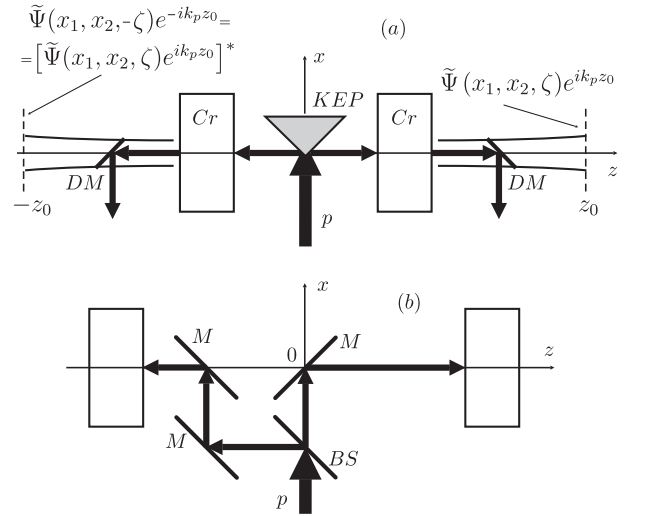


Figure 3: (a) a scheme for measuring the phase  $\varphi(x_1, x_2; \zeta)$  of the wave function  $\tilde{\Psi}(x_1, x_2; \zeta)$ ;  $KEP$  in 3a is the knife-edge prism splitting the pump ( $p$ ) for two equal counter-propagating parts, two rectangles describe two identical nonlinear crystals  $Cr$ .  $DM$  are the dichroic mirrors;  $z_0$  and  $-z_0$  are two observation planes,  $k_p = 2\pi/\lambda_p$ ; the part 3b shows how the  $KFP$  can be substituted by the beamsplitter  $BS$  and a series of mirrors  $M$ .

In this scheme the pump is assumed to be split for two equal counter-propagating parts directed each into its

own of two identical nonlinear crystals. Emitted photons from these crystals propagate in opposite directions of the  $z$ -axis, and they are characterized by the wave functions indicated in the picture of Fig. 3a. In accordance with Eq. (38), they are equal to  $|\tilde{\Psi}(x_1, x_2; \zeta)\rangle e^{\mp i\varphi(x_1, x_2; \zeta) \mp k_p z_0}$ , correspondingly, for the left and right parts of the picture.

The further analysis can be based on the well-known 4-photon Hong-Ou-Mandel effect [18? –20]. Continuation of the measurement scheme of Fig. 3 is shown in Fig. 4. Photons are assumed to be extracted by narrow pieces of fibers capturing only photons with more or less given coordinates,  $x_1$  or  $x_2$ . Then photons from the left- and right-hand shoulders of the scheme in Fig. (3) are sent to different sides of the beamsplitter, as shown in the picture of Fig. 4. Optical pathways of all routes have to be equalized. The total state vector of all 4 photons coming to  $BS$  will have the form

$$|\Psi_{in}\rangle = |\tilde{\Psi}(x_1, x_2, \zeta)\rangle \left\{ |e^{-i[k_p z_0 + \varphi(x_1, x_2)]} a_{x_2, u}^\dagger a_{x_1, l}^\dagger + e^{i[k_p z_0 + \varphi(x_1, x_2)]} a_{x_1, u}^\dagger a_{x_2, l}^\dagger \right\} |0\rangle, \quad (39)$$

where the subscripts “ $u$ ” and “ $l$ ” indicate the upper and lower sides of the  $BS$ . The BS transformation rules for the creation operators are

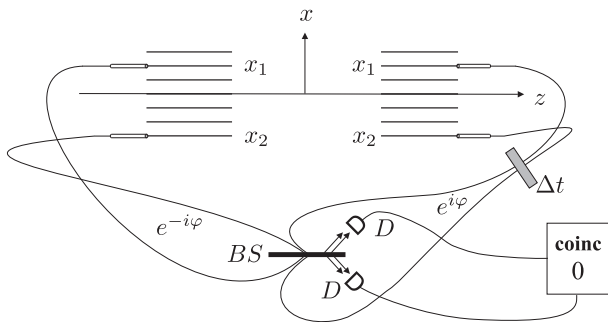


Figure 4: A scheme for extracting photons and measuring the phase via the interference HOM effect;  $BS$  and  $D$  indicate beamsplitter and detectors

$a_u^\dagger \rightarrow \frac{1}{\sqrt{2}}(a_u^\dagger + a_l^\dagger)$  and  $a_l^\dagger \rightarrow \frac{1}{\sqrt{2}}(a_u^\dagger - a_l^\dagger)$ . After BS photons can propagate in pairs either up or down, but also they can be split between the upper and lower half-planes. The state vector of this split part of photons is easily found to be given by

$$|\tilde{\Psi}_{out, split}\rangle = -i|\tilde{\Psi}(x_1, x_2; \zeta)\rangle \times \sin[k_p z_0 + \varphi(x_1, x_2)] \left[ a_{x_1, u}^\dagger a_{x_2, l}^\dagger - a_{x_1, l}^\dagger a_{x_2, u}^\dagger \right] |0\rangle. \quad (40)$$

In general,  $k_p z_0 + \varphi(x_1, x_2) \neq 0$ , which provides a nonzero coincidence signal between the higher and lower half-planes after BS. But the argument of sinus in Eq. (40) can be zeroed with the help of appropriately added delay time  $\Delta t$  for photons coming to  $BS$  either from the left or right pairs of extracted photons in Fig. 4. For

the case shown explicitly in this picture  $|\tilde{\Psi}_{out, split}\rangle$  the factor  $\sin[\dots]$  in Eq. (40) takes the form

$$\sin[k_p z_0 + \varphi(x_1, x_2) - \omega_p \Delta t]. \quad (41)$$

Evidently, both the function  $\sin[\dots]$  and  $|\tilde{\Psi}_{out, split}\rangle$  turn zero at

$$\omega_p \Delta t(x_1, x_2) - [k_p z_0 + \varphi(x_1, x_2)] = n\pi, \quad (42)$$

which corresponds to the zero coincidence signal for photons transmitted through and reflected from the beam-splitter. The closest to zero value of  $\Delta t(x_1, x_2)$  providing fulfillment of the condition (42) can be found experimentally by tuning the delay time until achieving the zero minimum of the coincidence signal. Then Eq. (42) can be used for finding the phase of the biphoton wave function for any given values of the variables  $x_1$  and  $x_2$ .

The described procedures of measurements of the phases and absolute values of the wave function should be repeated many times with varying values of variables  $x_1$  and  $x_2$ , after which the accumulated data have to be used for reconstruction of the searched elements of the reduced density matrix  $\rho_r(x_1, -x_1; \zeta)$  (20).

Of course, this is a very laborious and time-consuming work but, in principle, it seems to be doable.

## 5. DISCUSSION

As shown above, characterization of the degree of transverse entanglement in photon's coordinates differs significantly in approaches using the wave function or the reduced density matrix, and the question is why. A quick answer is because these two approaches describe in fact different types of correlations and entanglement. Characterization using wave functions describes correla-

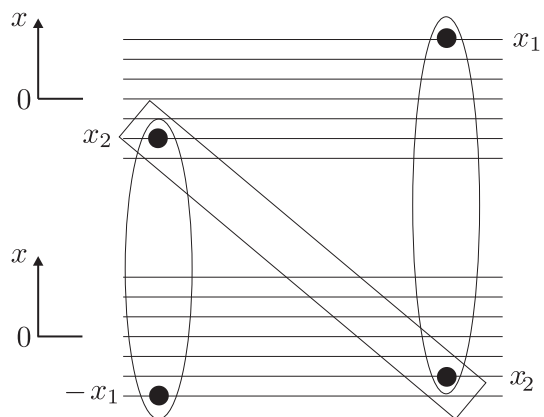


Figure 5: Two-channel propagations of photons after the beamsplitter and correlations between pairs of photons

tions between particles or variables inside single biphoton pairs, whereas the approach based on the reduced density matrix characterizes correlations between two different

pairs of photons. This last interpretation can be illustrated by the picture of Fig. 5. In this picture fat dots correspond to photon's coordinates and each of two ovals corresponds to a pair of simultaneously born photons. Two ovals correspond to two different pairs of photons which could be born at different atoms in the crystal and not simultaneously. But they are assumed to be coming simultaneously to detectors. One of the ovals is shown shifted compared to another one along the horizontal axis only for convenience of drawing but in fact, as said above, both pairs are assumed to arrive to detectors simultaneously. Definitely, photons in each pair are strongly correlated to each other because of simultaneity of their birth. But no correlations between pairs is expected to occur unless such correlations are specially imposed. In the case under consideration obstruction of correlations arises owing to the assumption of coinciding coordinates  $x_2$  in two pairs of photons which is shown by the rectangle in fig. 5. This obstruction provides correlations between the remaining coordinates  $x_1$  and  $-x_1$  of two different pairs. Thus, the arising in this case entanglement is related to correlations between pairs of photons rather than to photon-photon correlations in individual pairs. Interesting enough, just this type of correlations between pairs of photons provides the correct parameter of the degree

of entanglement  $R_{new}$  (33) valid in the coordinate representation both in and beyond the near zone, rather than the traditionally considered photon-photon correlations and the parameter  $R_x$  (24).

## 6. CONCLUSION

As a resume, a new definition is suggested for the parameter  $R_{new}$  (33) characterizing the degree of transverse entanglement and given by the ratio of widths of two single-particle distributions  $\rho_r(x_1, x_1)$  and  $\rho_r(x_1, -x_1)$ , with  $\rho_r(x_1, x'_1)$  being the reduced density matrix of the biphoton state in the coordinate representation. For the model double-Gaussian biphoton wave function the parameter  $R_{new}$  is found to be compatible with the Schmidt entanglement quantifier  $K$  both in and beyond the near zone of propagation of photons after their formation in the nonlinear crystal. Extension of the theoretical analysis for the case of the biphoton wave function free from Gaussian modeling remains strongly desirable. as well as the direct experimental measurement of the reduced density matrix  $\rho(x_1, -x_1; \zeta)$  (37). We hope to return to these problems elsewhere.

- 
- [1] R. S. Thebaldi S. P. Walborn, A. N. de Oliveira and C. H. Monken. *Phys. Rev. A*, 69:023811, 1994.
- [2] C. K. Law and J. H. Eberly. *Phys. Rev. Lett.*, 92:127903, 2004.
- [3] M. A. Efremov M.V. Fedorov, S. S. Straupe P. A. Volkov, E. V. Moreva, and S. P. Kulik. *Phys. Rev. Lett.*, page 063901, 2007.
- [4] M. V. Fedorov and N. I. Miklin. *Contemporary physics*, 55:94, 2014.
- [5] K. Rzazewski R. Grobe and J. H. Eberly. *J. Phys. B*, 27:L503, 1994.
- [6] P. A. Volkov M. V. Fedorov, M. A. Efremov and J. H. Eberly. *J. Phys. B*, 39:S467, 2006.
- [7] A. E. Kazakov K. W. Chan C. K. Law M. V. Fedorov, M. A. Efremov and J.H. Eberly. *Phys. Rev. A*, 69:052117, 2007.
- [8] J. P. Torres K. W. Chan and J. H. Eberly. *Phys. Rev. A*, 75:050101(R), 2007.
- [9] M V Chekhova F Just, A Cavanna and G Leuchs. *New J. Phys.*, 15:083015, 2013.
- [10] M. G. Raymer A. I. Lvovsky. *Rev. Mod. Phys*, 81:299, 2009.
- [11] I. A. Walmsley E. Mukamel, K. Banaszek. *Optics Lett.*, 28:2003, 2015.
- [12] M. G. Raymer I. A. Walmsley K. Banaszek B. J. Smith, B. Killett. *Optics Lett.*, 30:3365, 2005.
- [13] F. Toscano P. H. Souto Ribeiro S. P. Walborn D. S. Tasca, R. M. Gomes. *Phys. Rev. A*, 83:052325, 2011.
- [14] Wei Song Ping Zou, Zhi-Ming Zhang. *Phys. Rev. A.*, 91:052109.
- [15] Y. Chalich M. J. Horton J. Banker G. S. Thekkadath, L. Giner and J. S. Lundeen. *Phys. Rev. Lett.*, 117:120401, 2018.
- [16] A. A. Clerk O. Landon-Cardinal, L. C. G. Govia. *Phys. Rev. Lett.*, 120:090501, 1961.
- [17] D. Dequal P. Villoresi G. Vallone L. Calderaro, G. Fioletto. *Phys. Rev. Lett.*, 121:230501, 2018.
- [18] Z. Y. Ou C. K. Hong and L. Mandel. *Phys. Rev. Lett.*, 59:2044, 1987.
- [19] S. V. Vintskevich M. V. Fedorov, A. A. Sysoeva and D. A. Grigoriev. *Phys. Rev. A*, 98:013850, 2018.
- [20] C. Silberhorn A. Ferreri, V. Ansari and P. R. Sharapova. *Phys. Rev. A.*, 100:053829, 2019.